The Astrophysical Journal, 617:1323–1329, 2004 December 20

ASTROMETRIC DISCOVERY OF GJ 164B

Steven H. Pravdo
Jet Propulsion Laboratory, California Institute of Technology, MS 306-431, 4800 Oak Grove Drive, Pasadena, CA 91109; spravdo@jpl.nasa.gov

Stuart B. Shaklan
Jet Propulsion Laboratory, California Institute of Technology, MS 301-486, 4800 Oak Grove Drive, Pasadena, CA 91109; shaklan@huey.jpl.nasa.gov

Todd Henry
Department of Physics and Astronomy, Georgia State University, Atlanta, GA 30302-4106; thenry@chara.gsu.edu

and

G. Fritz Benedict
MacDonald Observatory, University of Texas at Austin, Austin, TX 78712-1083; fritz@astro.as.utexas.edu
Received 2004 July 9; accepted 2004 September 1

ABSTRACT

We discovered a low-mass companion to the M dwarf GJ 164 with the CCD-based imaging system of the Stellar Planet Survey astrometric program. The existence of GJ 164B was confirmed with *Hubble Space Telescope* NICMOS imaging observations. A high-dispersion spectral observation in V sets a lower limit of $\Delta m > 2.2$ mag between the two components of the system. Based on our parallax value of 82 ± 8 mas, we derive the following orbital parameters: $P = 2.04 \pm 0.03$ yr, $a = 1.03 \pm 0.03$, and $M_{\rm total} = 0.265 \pm 0.020\ M_\odot$. The component masses are $M_A = 0.170 \pm 0.015\ M_\odot$ and $M_B = 0.095 \pm 0.015\ M_\odot$. Based on its mass, colors, and spectral properties, GJ 164B has spectral type M6–M8 V.

Subject headings: astrometry — stars: individual (GJ 164B) — stars: low-mass, brown dwarfs

Online material: color figures

1. INTRODUCTION

M dwarfs are a large population of stars that have not yet been systematically searched for low-mass companions, both planets and brown dwarfs. Of the ~100 extrasolar planets known (Marcy & Butler 2000; Butler et al. 2002 and references therein), only one system, GJ 876, has an M dwarf primary (Marcy et al. 1998, 2001; Delfosse et al. 1998). It is too early to conclude whether this low fraction is real or a selection effect.

We astrometrically search for low-mass companions to selected M dwarfs with the Stellar Planet Survey (STEPS; Pravdo & Shaklan 1996). As expected, we are detecting the largest mass companions with the largest signals first, and we expect to detect smaller mass companions down to a limit of $\sim M_{\rm J}$ as the baselines and sensitivities increase. Pravdo & Shaklan (2003) reported the detection of a low-mass companion to GJ 1245A, GJ 1245C (Harrington & Dahn 1984; McCarthy et al. 1988; Harrington 1990), with a mass of $\sim 0.07\ M_\odot$ (Henry et al. 1999). Here we report the discovery of another low-mass companion around a nearby M star, GJ 164. GJ 164, also known at LHS 1642 and Ross 28, is 11–13 pc distant (van Altena et al. 1995, hereafter YPC) with $V = 13.5$ (Weis 1996).

2. OBSERVATIONS, ANALYSIS, AND RESULTS

2.1. *STEPS Astrometry*

2.1.1. *STEPS Instrument and Program*

The STEPS instrument is mounted at the Cassegrain focus of the Palomar 200 inch (5.08 m) telescope, with an f/16 beam incident on an LN_2-cooled, 4096×4096, 15 μm pixel CCD camera. The dewar window is optically flat (<1/30 wave peak-to-valley) to limit optical distortions and also serves as a filter in the 550–750 nm band to limit color effects. The plate scale is 36 mas pixel^{-1}, resulting in a field 2.′45 on a side. We sum 2×2 physical pixels on a chip to reduce the readout time to ~7 s via four output amplifiers after each 30–60 s exposure. This is acceptable because the ~1″ point-spread functions (PSFs) are significantly oversampled.

STEPS began in 1997 with the current instrument and continues with 30 program stars. We observe ~12 nights yr^{-1} spread over most of the year except for March–June, when our targets are inaccessible. Seasonal patterns of bad weather have greatly affected the temporal sampling. The STEPS targets are all nearby M dwarfs, fainter than $V \sim 12$ to avoid saturation and at a low enough Galactic latitude to have a sufficient number ($\geq$6) of reference stars in the field. Measurement noise is comprised of Poisson noise and systematic noise due to color differences between the target and reference stars (differential chromatic refraction [DCR]) and variability in the atmosphere, telescope optics, camera electronics, and CCD geometry. These are discussed in the Appendix (see also Pravdo & Shaklan 1996). The current noise floor is ~1 mas, somewhat above the theoretically expected value of ~0.5 mas.

2.1.2. *Astrometric Modeling*

We use in-frame relative astrometry to find stellar companions via the wobble of the primary around the center of mass. The model is a two-dimensional linear model of the form

$$x' = c_1 + c_2 x + c_3 y,$$
$$y' = c_4 + c_5 x + c_6 y, \quad (1)$$

where (x, y) are raw coordinates, (x', y') are fitted coordinates, and the c_i are the six coefficients of the fit.

The signal of a companion is first revealed as a periodic residual after the much larger motions due to parallax and proper motion are removed from each target motion. We then use the nonlinear Marquardt routine (Press et al. 1989, p. 523) to fit the total motion to a model with 14 possible parameters: seven orbital elements, two proper motion components, one parallax, two celestial position components at an epoch, one radial velocity, and a parameter that depends on the light ratio in the "high-mass" branch ($M_{\rm comp} \geq 0.08\ M_\odot$) or on the mass ratio in the "low-mass" branch ($M_{\rm comp} < 0.08\ M_\odot$). In practice, the mean anomaly is set to zero at the derived epoch, and the celestial positions and radial velocity are fixed, since the model is insensitive to small changes in their values, leaving 10 free parameters. The multidimensional χ^2 space is quite complex, and we use a Monte Carlo program that explores the parameter space in conjunction with the Marquardt routine. Uncertainties of 1 σ are calculated with the method of Lampton et al. (1976) for parameter estimation in multidimensional models.

We observe the movement of the center of light around the center of mass: the photocentric orbit. In the limit at which the companion light is negligible, this is the same as the Keplerian orbit of the primary. However, when the companion makes a significant contribution to the light via self-luminosity, the orbit of the photocenter is reduced, and it approaches the limit of zero motion when the companion and the primary have the same mass and light. Therefore, for a given observed motion, there are two possible solutions. If we detect a small motion of the primary, it could be due to either a relatively small-mass, nonluminous secondary or a relatively large-mass, luminous secondary. Distinguishing between the two possibilities requires imaging or spectroscopic information.

The ratio of the photocentric and Keplerian orbits, α/a, is (e.g., McCarthy et al. 1988)

$$\alpha/a = f - \beta, \tag{2}$$

where f is the fractional mass of the secondary, β is the fractional light, a is the semimajor axis, and α is the photocentric radius. We use the visible mass-luminosity relation (MLR; Henry et al. 1999) to relate the absolute luminosity of each component to its mass. As the mass and absolute luminosity of the secondary decrease, β becomes negligible compared with f in equation (2), and the MLR also becomes inapplicable. This limit is reached at 0.08 $M_\odot$. Figure 1 plots f, β, and α/a as functions of the secondary mass for this system and also demonstrates that for each α/a value, aside from the maximum of $\sim$0.31, there are two possible secondary masses.

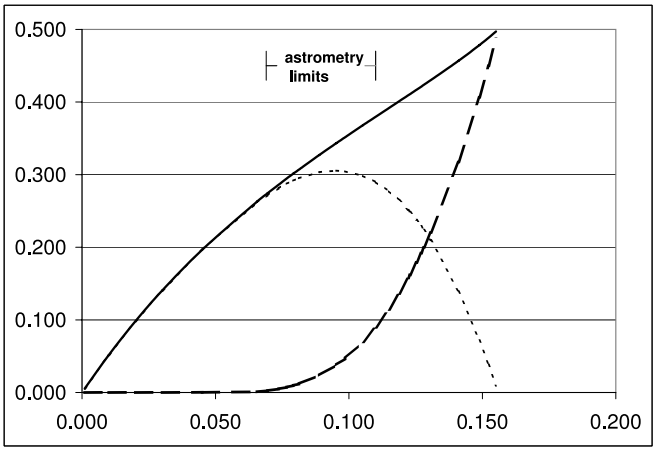

FIG. 1.—Fractional mass ratio f (*solid line*), fractional light ratio β (*dashed line*), and photocentric-to-relative orbit ratio α/a (*dotted line*) as functions of the GJ 164B mass. The range of acceptable astrometric fits is shown by the "astrometry limits." [*See the electronic edition of the Journal for a color version of this figure.*]

2.1.3. *GJ 164 Parallax and Proper Motion*

We determine parallax and proper motions relative to our reference frame. Our values may differ from the absolute values because the reference frame is not infinitely distant. The GJ 164 frame contains nine reference stars with an average in-band intensity of $\sim$1% of GJ 164, implying an average distance 10 times farther. In addition, in all cases the reference stars are bluer than GJ 164, implying earlier spectral types, higher luminosities, and even larger distances. The effects of absorption and reddening at this Galactic latitude, $\sim 1^\circ$, must also be taken into account. We use here a standard correction as described in § 2.1.4. However, we use our relative values in our astrometric fits because they are appropriate for removing these motions in our data. In determining the final system parameters, we allow for an absolute parallax value that differs from our fitted value.

TABLE 1
GJ 164 PROPERTIES

PARAMETER	LITERATURE	REFERENCES	THIS WORK	
			Primary	Secondary
R.A. (FK5 2000/J2000.0).....	04 12 58.94	Bakos et al. (2002)	...	...
Decl. (FK5 2000/J2000.0).....	52 36 40.7	Bakos et al. (2002)	...	...
Proper motion (arcsec).....	0.910	Luyten (1979)	0.871 ± 0.002	...
P.A. (deg).....	203.7	Luyten (1979)	201.9 ± 0.1	...
Relative parallax (mas).....	...		71^{+4}_{-2}	...
Absolute parallax (mas).....	83.9 ± 8.7	YPC	82 ± 8	...
M_V[a].....	13.10	Weis (1996)	<13.23	>15.43
M_J[a].....	8.37	2MASS	8.48	10.62
M_H[a].....	7.84	2MASS	7.92	10.42
M_{K_s}[a].....	7.51	2MASS	7.65	9.63
Spectral type[a].....	M4.5 V	Reid et al. (1995)	M4.5 V	M6–M8 V

NOTE.—Units of right ascension are hours, minutes, and seconds, and units of declination are degrees, arcminutes, and arcseconds.

[a] For $\Pi = 82$ mas.

TABLE 2
ORBITAL PARAMETERS

Parameter	From Astrometry	Plus Imaging and Spectroscopy
Period (yr)	2.04 ± 0.03	...
Semimajor axis (AU)	1.02 ± 0.05	1.03 ± 0.03
Eccentricity	$0.2^{+0.3}_{-0.2}$	...
Inclination (deg)	120 ± 12	...
Longitude of ascending node (deg)	258 ± 14[a]	...
Argument of periapse (deg)	300[a, b]	...
Epoch	1998.8[b]	...
Total mass ($M_\odot$)	0.255 ± 0.030	0.265 ± 0.020
GJ 164A mass ($M_\odot$)	0.170 ± 0.020	0.170 ± 0.015
GJ 164B mass ($M_\odot$)	0.085 ± 0.030	0.095 ± 0.015

[a] Or 78° longitude of the ascending node and 120° argument of the periapse because of the ambiguity of being in or out of the plane of the sky.
[b] Not meaningfully constrained, since orbit could be circular.

The literature contains several values for both the proper motion and parallax of this star. The Revised Luyten Half-Second (LHS) catalog (Bakos et al. 2002) has -284 mas yr^{-1} in right ascension and -854 mas yr^{-1} in declination, the LHS catalog (Luyten 1979) has -366 mas yr^{-1} in right ascension and -833 mas yr^{-1} in declination, and Heintz (1993) gives -320 mas yr^{-1} in right ascension and -811 mas yr^{-1} in declination.

Three previously determined trigonometric parallax values are 63 ± 10 mas (van Maanen 1931), 78.2 ± 8.2 mas (Hershey 1980), and 86.8 ± 6.7 mas (Heintz 1993). These are combined to yield a weighted average for the absolute parallax of 83.9 ± 8.7 mas (YPC). We suggest that the variation among the prior results was caused in part by an interaction with the proper motion values, which are also significantly divergent, with the underlying cause being the time-dependent, unaccounted-for contribution of the companion.

2.1.4. *GJ 164 Results*

We have now observed GJ 164 with STEPS from 1997 December 19 to 2004 February 17, or for more than 6 years. During that time GJ 164 moved ~2000 mas in right ascension and ~5000 mas in declination as a result of its proper motion. If we fit our data without a companion we get a parallax of 73 mas and proper motions of -322 mas yr^{-1} in right ascension and -808 mas yr^{-1} in declination, the latter being consistent with prior results. The addition of GJ 164B to the model fit changes our results only slightly.

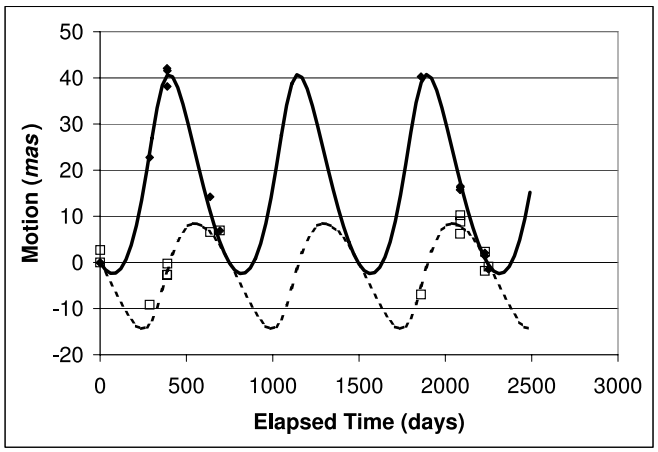

FIG. 2.—R.A. and decl. relative motion of the GJ 164 photocenter measured with STEPS. The points show the data (R.A.: *diamonds*; decl.: *squares*), and the lines (R.A.: *solid*; decl.: *dashed*) show the 2.04 yr model with a 0.10 $M_\odot$ secondary. Errors on the points are 2 mas. [*See the electronic edition of the Journal for a color version of this figure.*]

The addition of a companion to the total motion model significantly reduces the residuals in the fit from ~18 to ~2 mas. The ~2 mas residual is larger than the ≤ 1 mas residuals we achieve in other data sets and is due to either other real motion in the system or systematic error. Tables 1 and 2 give our best-fit values for the orbital parameters, relative parallax, and proper motion. Figure 2 shows a fit of the residuals to a model with a companion in a 2.04 yr period after parallax and proper motion subtraction. A ~4 yr orbital period also fits these data because of the uncertainty introduced by the ~1000 day data gap but is less likely to be correct based on other information (see below). For GJ 164 the low- and high-mass branches of the model merge, since the orbit ratio (α/a) is near ~0.31 (Fig. 1). In our fits, $\alpha/a = 0.289 \pm 0.017$, $f = 0.32 \pm 0.06$, and $\beta = 0.046 \pm 0.044$.

Our relative parallax, 71^{+4}_{-2} mas, falls among the prior results. To correct this to the absolute parallax, we add 2 mas, typical for stars of this magnitude and Galactic latitude (YPC, Fig. 2), yielding 73^{+4}_{-2}. However, our imaging and spectroscopic results, if we assume that GJ 164A is well described by the visible and near-infrared MLRs, imply a larger value for the parallax (see § 3).

2.2. *Hubble Space Telescope Imaging*

We performed observations with the NICMOS 1 camera of the *Hubble Space Telescope* (*HST*) on 2003 December 23 and 2004 February 14, using the F108N and F190N filters at a fixed, arbitrary roll angle on the first date and the F108N, F164N, and F190N filters at a fixed roll angle of 45° from the first roll angle on the second date, for a total of five observations. The observations were dithered in a spiral pattern with a 0.″445 step size to smooth pixel effects. We searched for a faint companion to GJ 164A in two ways. First, we subtracted the pipeline-processed mosaicked images with the same filter and different roll angles to eliminate persistent effects such as the image of the primary and any other azimuthally constant features. Second, we used the PSFs in TinyTim[1] to create a model of two point sources representing components A and B. We used this model to fit the five observations with relative flux, separation, and position angle (P.A.) as the free parameters. Figure 3 shows

[1] See http://www.stsci.edu/software/tinytim/tinytim.html.

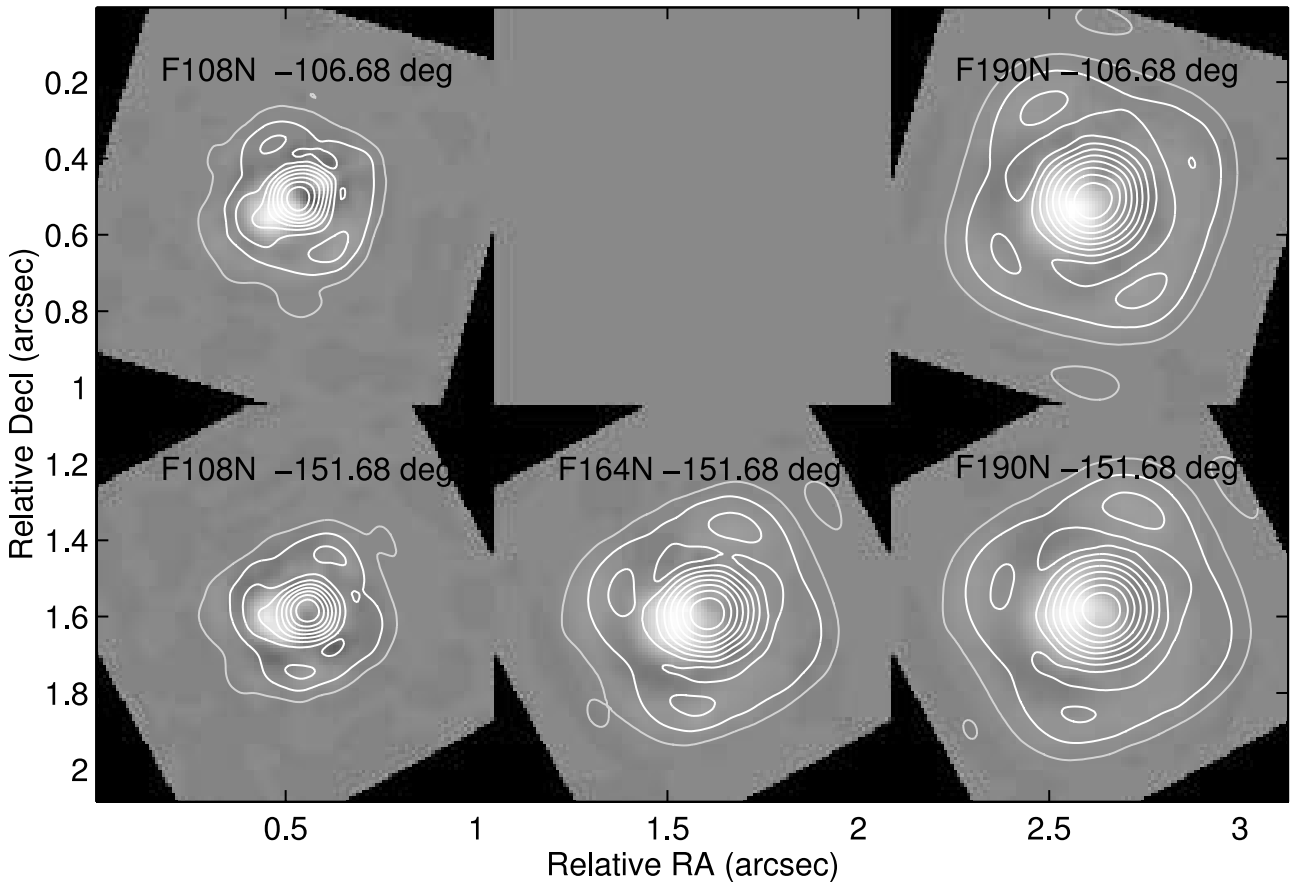

FIG. 3.—Five *HST* images with the TinyTim PSF of GJ 164A subtracted. The top two images are from the first date (initial roll angle and two filters), and the bottom three are from the second date, 53 days later (second roll angle and three filters). The contours represent light levels including GJ 164A.

the resulting images after subtraction of component A, and Tables 3 and 4 list the results. We include in Table 1 an approximate guide to the relative fluxes of the components in *JHK*, acknowledging that the narrow *HST* filter bands are only rough approximations, with F164N perhaps the best match, as it is well centered in *H*.

The most important result seen in all five images is the confirmation of the existence of the astrometric companion, GJ 164B. The companion is to the southeast in the December images and to the east in February. GJ 164B cannot be a stationary background object because it would have appeared to move northeast as GJ 164A's proper motion carried it southwest. If it were stationary, it would be 84 mas north of GJ 164A in the second observation, rather than the measured 15 mas south.

The *HST* positional data were represented in the STEPS format, i.e., a right ascension and declination positional offset at a Julian Date, and we fit the astrometric model to the STEPS and *HST* data simultaneously. The 2.04 yr astrometric orbit is a significantly better fit than a 4 yr model (2 mas compared with 3.4 mas residuals), resulting in values of 75 mas at P.A. = 114°, and 86 mas at P.A. = 101°, in good agreement with the *HST* observations (Table 3).

Table 4 shows the photometry for the three bands. The light ratios are about 6–7:1 in each band, with uncertainties of ~10%.

2.3. *Spectroscopy*

We searched for evidence that GJ 164 is a double-lined spectroscopic binary (SB2). The observations were made on 2004 February 12, with the Sandiford Cass Echelle spectrograph on the McDonald Observatory 2.1 m telescope. We used the IRAF task *fxcor* to cross-correlate the spectrum with a template high signal-to-noise spectrum of the M2.5 V J dwarf Gl 623 (Henry et al. 1994), obtained at the 9.2 m Hobby-Eberly Telescope. We consider Gl 623 to be an effectively "nonbinary" template because its two components differ by ~5.3 mag (Henry et al. 1999). Figure 4 shows a sample correlation function for one of the 22 echelle orders. It appears very sharp and symmetrical. A weighted average of the velocities from each of

TABLE 3
HST ORBITAL MEASUREMENTS

Date	Separation (mas)	P.A. (deg)
2003 Dec 12	75 ± 1	116 ± 3
2004 Feb 14	88 ± 3	100 ± 3

TABLE 4
HST FLUX RATIOS

Filter	Flux Ratio
F108N	0.14 ± 0.02
F164N	0.17 ± 0.01
F190N	0.17 ± 0.01

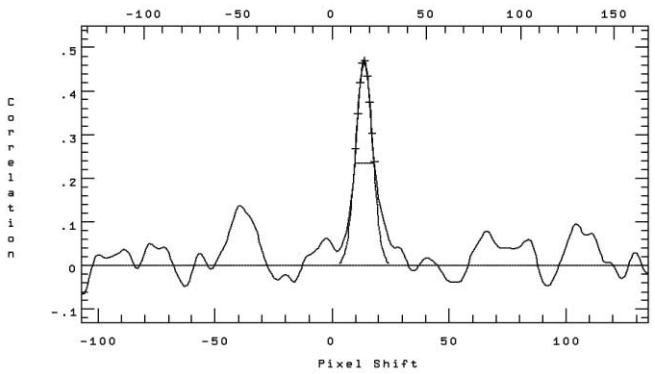

FIG. 4.—Cross-correlation function obtained for GJ 164, using a Gl 623 template. The spectral range for this particular order was 547–553 nm. The correlation peak is indistinguishable from that of a single star.

the 22 orders yields a radial velocity $V_r = -29.9 \pm 0.3$ km s^{-1} (heliocentric), where the velocity uncertainty in the ephemeris of our binary template has been included. We then attempted to deblend the eight cleanest correlation peaks but found no evidence of duplicity. We estimate that the V magnitude difference between components is at least 2.2. We base this limit on the previous successful analysis of Wolf 1062 (Gl 748), an SB2 with $\Delta m = 1.8$ (Benedict et al. 2001), and, in an ongoing investigation, on marginal detection of the two components of Wolf 922 (Gl 831; $\Delta m = 2.1$; Henry et al. 1999), but at periastron (largest ΔV_r). This would restrict the mass of the companion to be less than 0.11 $M_\odot$, confirming the astrometric upper limit (Table 2).

Figure 5 also shows the location in the orbit when the spectroscopic observation was made (circle on the plot). At that time, the estimated $\Delta V_r \sim 13$ km s^{-1}. Current extrasolar planet-finding radial velocity experiments should detect the motion of the $V \sim 13$ primary in this orbit.

3. DISCUSSION

The GJ 164 orbit as determined from astrometry is shown in Figure 5, in which we have taken the measured photocentric orbit of the primary and transformed it into an orbit that shows the motion of the secondary. We superpose on the plot the points in the orbit when we had *HST* and spectral observations. There is consistency between the astrometry and the imaging with respect to the position angles, the direction of motion, and the separation between the components.

Our imaging and spectroscopic measurements and the MLRs in the H (Henry & McCarthy 1993) and V (Henry et al. 1999) bands allow us to infer both the primary mass and the parallax, assuming that the primary is neither over- nor underluminous in H compared with V. Since the *HST* F164N measurement is narrow and centered in the H band, we take its ratio to be approximately equal to the H ratio. The F108N band is contained in J, and the F190N band is contained in the K band, but both are off center, so the ratios are probably less representative. Nevertheless, we use them for zeroth-order estimates of the JHK Δm (Table 1). We obtain upper limits to the primary mass (as a function of parallax) by assuming that all the visible light comes from the primary. Likewise, a lower limit is obtained by using the upper limit to the V-band Δm (§ 2.3). Next, we calculate H magnitudes for the primary from the H-band MLR, for these mass limits. The difference between the calculated H luminosity of the primary and the 2MASS value tells us the H magnitude of the secondary, and thus the secondary-to-primary ratio. This ratio is assumed to be equal to the F164N ratio. Parallax values less than 86 mas are not allowed, as they would result in H ratios that are too high. Similarly, parallax values more than 90 mas are not allowed, as they would result in H ratios that fall below the F164N ratio. Figure 6 shows the V-based limits (*solid lines*) and the H-based limits (*dotted lines*). The overlapping region constrains the parallax to be 86 ± 2 mas and the GJ 164A mass to be 0.163 ± 0.004 $M_\odot$, without considering the uncertainty in the MLR itself ($\geq$20%; see following). The F164N ratio and the H-based MLR then constrain $M_B \leq 0.092$ $M_\odot$ with an uncertain lower limit below 0.08 $M_\odot$, since the MLR is not valid in that range.

If the parallax is 86–90 mas rather than our corrected value of 73 mas, then the masses of the objects and the size of the orbit are smaller, while the period remains the same. The net effect is to reduce the orbital effect of the secondary by either lowering its mass or increasing its light. For parallaxes above 82 mas, the central portion of the secondary mass range, $M_B \sim 0.075$–0.10 $M_\odot$, is a slightly worse fit than before (3 rather than 2 mas

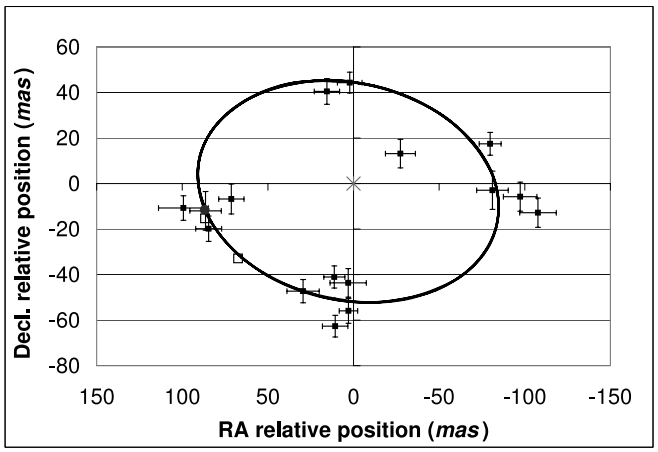

FIG. 5.—STEPS data points and errors superposed on the 2 yr astrometric orbital model of GJ 164B (*curve*) around GJ 164A (*asterisk*). We also show the positions at the times of the *HST* (*open squares*) and spectroscopic (*circle*) observations. [*See the electronic edition of the Journal for a color version of this figure*.]

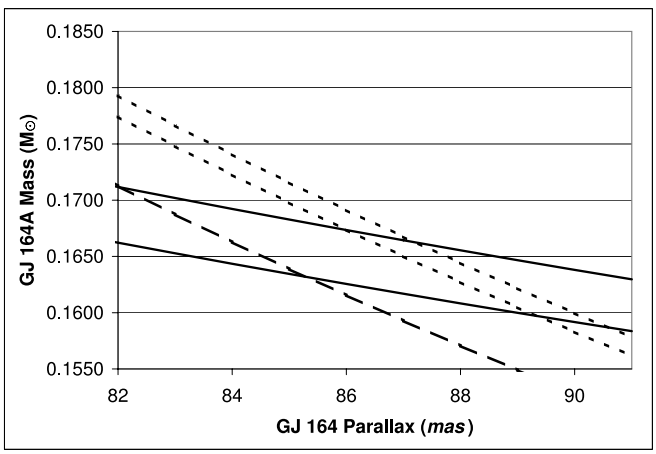

FIG. 6.—GJ 164A mass and parallax limits. The solid lines show the maximum mass based on the V-band MLR and the minimum mass based on the observed V-band Δm. The dotted lines show the limits imposed on the mass by the *HST* F164N light ratio and the H-band MLR. The dashed line corresponds to a GJ 164B/GJ 164A H luminosity ratio of 0.25. [*See the electronic edition of the Journal for a color version of this figure*.]

residuals). However, we do not believe that $M_B < 0.075\ M_\odot$, based on the inferred *JHK* values. The other possibility, $M_B > 0.10\ M_\odot$, is inconsistent with $M_B < 0.092\ M_\odot$ based on the *H* magnitudes analysis above. This inconsistency would be eliminated, however, if the *H* ratio between the components were 0.25 (Fig. 6, *dashed line*) rather than 0.17 ± 0.01 or if the primary mass were 0.177 rather than 0.167 $M_\odot$, corresponding to a difference in the *V*-band MLR of 0.28 mag in M_V. This last possibility is not unreasonable, since 0.28 is less than the 0.5–1.0 mag spread expected for stars of this mass with varying metallicity (Baraffe et al. 1998). Our estimate for the absolute parallax is thus 82 ± 8 mas. The primary and secondary mass estimates are then $M_A = 0.170 \pm 0.015\ M_\odot$ and $M_B = 0.095 \pm 0.015\ M_\odot$.

The likely stellar type of GJ 164B is M6–M8, with the uncertainty due mostly to the parallax. A similar star might be GJ 644C (Henry et al. 2004), classified as M7.0 V with M_J, M_H, and M_{K_s} equal to 10.73, 10.15, and 9.77, respectively, while GJ 164B has 10.62, 10.42, and 9.63 (Table 1).

There has been no sensitive X-ray observation of GJ 164; an upper limit of $\sim 8 \times 10^{27}$ ergs s^{-1} can be inferred during the epoch of the *ROSAT* survey (Hünsch et al. 1999). This does not place significant constraints on whether GJ 164 is "X-ray active," although the lack of significant Hα emission is associated with low coronal X-ray emission (Doyle 1989) and with older, slower rotators. An age estimate based on the $V - I_C$ color method (Hawley et al. 1999; Gizis et al. 2002) yields $\sim$2.5 billion yr.

4. CONCLUSION

We have astrometrically discovered a low-mass companion to GJ 164A and confirmed the discovery with imaging. Future observations will reduce the uncertainties in the GJ 164B mass, type, and age and will allow us to further explore the properties of stars in this difficult-to-observe mass region.

The research described in this paper was performed in part by the Jet Propulsion Laboratory, California Institute of Technology, under contract with the National Aeronautics and Space Administration. We performed observations at Caltech's Palomar Observatory and acknowledge the assistance of the staff. This research has made use of the NASA/IPAC Infrared Science Archive, which is operated by the Jet Propulsion Laboratory, California Institute of Technology, under contract with the National Aeronautics and Space Administration. This research has made use of the SIMBAD database, operated at CDS, Strasbourg, France, and of the NASA Astrophysics Data System abstract service. This publication makes use of data products from the Two Micron All Sky Survey, which is a joint project of the University of Massachusetts and the Infrared Processing and Analysis Center, California Institute of Technology, funded by the National Aeronautics and Space Administration and the National Science Foundation. We also acknowledge use of the NStars Database. We thank the referee W. van Altena for useful suggestions.

APPENDIX

The data reduction process begins by extracting square regions containing the target and reference stars from the raw frames and organizing them into a single file. If desired, the corresponding regions from flat-field files are also extracted for use in the centroiding step.

Next, the positions for all stars are determined. Our algorithm measures the cross-correlation of the reference stars relative to the target. The cross-correlation is determined by the weighted slope of the phase of the Fourier Transform of the images after summing them into horizontal and vertical distributions. The algorithm has several advantages compared to traditional techniques. Standard centroids and Gaussian fits are sensitive to the background level and shape of the PSF. Our algorithm is insensitive to the background level and robust against changes in the shape of the PSF and maintains a signal-to-noise ratio comparable to matched filtering.

We form a preliminary astrometric solution after centroiding by fitting a conformal six-term (three per axis) transformation for each CCD frame to a reference frame. The transformation is then applied to the target star, allowing the target star position to be measured relative to the surrounding reference stars.

An automated frame-editing program searches for frames whose astrometric noise is above a user-defined threshold. Generally, the threshold is very high (20 σ) because the major cause of unusable data is missing reference stars or the selection of the wrong star. After frame removal, the conformal transformation is rerun to form an intermediate astrometric solution.

Because the stars do not all have the same effective color, they are affected by DCR. The DCR amplitude is as large as $\sim$10 mas for our bandpass and range of zenith distances. The effect is proportional to the tangent of the zenith angle and manifests itself as a linear drift in right ascension and a parabolic shift (relative to the meridian position) in declination. The relative DCR coefficient for each star is determined by fitting the right ascension drift. A single coefficient is determined for each star as the weighted average of the nightly coefficients.

The centroid positions are then adjusted to account for DCR, and the conformal transformation is rerun. All observations are made within 1.5 hr of meridian transit to minimize chromatic effects. At this point, the motion of the target star relative to the reference frame is known and plotted. Nightly statistics are computed, and the mean position and time of observation are written to a file.

The final processing step is to fit the motion of the target star to a model that contains the parallax, proper motion, and radial velocity of the target stars and the effect of any companion. Note that we determine and use the relative, rather than absolute, proper motions and parallaxes. In practice, the model is insensitive to radial velocity, but we input its fixed value when known. We use the USNO subroutine ASSTAR to compute the astrometric place of the star from its mean place, proper motion, parallax, and radial velocity and the NAIF subroutine CONICS to determine the state (position, velocity) of the orbiting body from a set of elliptic orbital elements.

REFERENCES

Bakos, G. A., Sahu, K. C., & Nemeth, P. 2002, ApJS, 141, 187
Baraffe, I., Chabrier, G., Allard, F., & Hauschildt, P. H. 1998, A&A, 337, 403
Benedict, G. F., et al. 2001, AJ, 121, 1607
Butler, R. P., et al. 2002, ApJ, 578, 565
Delfosse, X., Forveille, T., Mayor, M., Perrier, C., Naef, D., & Queloz, D. 1998, A&A, 338, L67
Doyle, J. G. 1989, A&A, 218, 195
Gizis, J. E., Reid, I. N., & Hawley, S. L. 2002, AJ, 123, 3356

Harrington, R. S. 1990, AJ, 100, 559
Harrington, R. S., & Dahn, C. C. 1984, IAU Circ. 3989
Hawley, S. L., Reid, I. N., & Gizis, J. E. 1999, in Very Low Mass Stars and Brown Dwarfs, ed. R. Rebolo & M. R. Zapatero-Osorio (Cambridge: Cambridge Univ. Press), 109
Heintz, W. D. 1993, AJ, 105, 1188
Henry, T. J., Franz, O. G., Wasserman, L. H., Benedict, G. F., Shelus, P. J., Ianna, P. A., Kirkpatrick, J. D., & McCarthy, D. W., Jr. 1999, ApJ, 512, 864
Henry, T. J., Kirkpatrick, J. D., & Simons, D. A. 1994, AJ, 108, 1437
Henry, T. J., & McCarthy, D. W., Jr. 1993, AJ, 106, 773
Henry, T. J., Subasavage, J. P., Brown, M. A., Beaulieu, T. D., Jao, W.-C., & Hambly, N. C. 2004, AJ, 128, 2460
Hershey, J. L. 1980, AJ, 85, 1399
Hünsch, M., Schmitt, J. H. M. M., Sterzik, M. F., & Voges, W. 1999, A&AS, 135, 319
Lampton, M., Margon, B., & Bowyer, S. 1976, ApJ, 208, 177
Luyten, W. J. 1979, A Catalogue of Stars with Proper Motions Exceeding 0″.5 Annually (Minneapolis: Univ. Minnesota)
Marcy, G. W., & Butler, R. P. 2000, PASP, 112, 137
Marcy, G. W., Butler, R. P., Fischer, D., Vogt, S. S., Lissauer, J. J., & Rivera, E. J. 2001, ApJ, 556, 296
Marcy, G. W., Butler, R. P., Vogt, S. S., Fischer, D., & Lissauer, J. J. 1998, ApJ, 505, L147
McCarthy, D. W., Jr., Henry, T. J., Fleming, T. A., Saffer, R. A., Liebert, J., & Christou, J. C. 1988, ApJ, 333, 943
Pravdo, S. H., & Shaklan, S. B. 1996, ApJ, 465, 264
———. 2003, in ASP Conf. Ser. 294, Scientific Frontiers in Research on Extrasolar Planets, ed. D. Deming & S. Seager (San Francisco: ASP), 107
Press, W., Flannery, B. P., Teukolsky, S. A., & Vetterling, W. T. 1989, Numerical Recipes (Cambridge: Cambridge Univ. Press)
Reid, I. N., Hawley, S. L., & Gizis, J. E. 1995, AJ, 110, 1838
van Altena, W. F., Lee, J. T., & Hoffleit, E. D. 1995, The General Catalogue of Trigonometric Parallaxes (4th ed.; New Haven: Yale Univ. Obs.) (YPC)
van Maanen, A. 1931, Mt. Wilson Contrib. 435
Weis, E. 1996, AJ, 112, 2300